Modern Physics Letters A

The discovery of two new surprising D_s states.

Antimo Palano

INFN and University of Bari,
Via Orabona 4, Bari, 70126, Italy.
antimo@ba.infn.it

The *BABAR* experiment has discovered an unexpected new narrow state, $D^*_{sJ}(2317)^+$ in the inclusive $D_s^+\pi^0$ invariant mass distribution from e^+e^- annihilation data at energies near 10.6 GeV. The same experiment has also shown evidence for structure in the 2.46 GeV/c^2region in the $D_s^*(2112)^+\pi^0$ mass spectrum. These discoveries have triggered a search in several experiments for new states coupled to the D_s^+ meson which have confirmed the existence of $D^*_{sJ}(2317)^+$ together with $D_{sJ}(2458)^+ \to D_s^*(2112)^+\pi^0$ both in inclusive e^+e^- annihilation and in B decays. These two new states are difficult to explain in terms of potential models.

Keywords: Charmed mesons; strange mesons; spectroscopy; BaBar.

PACS Nos.: 14.40.Lb, 13.25.Ft, 12.40.Yx

1. Introduction

The recent and unexpected discovery by the *BABAR* experiment of a narrow state, $D^*_{sJ}(2317)^+ \to D_s^+\pi^0$ [1], and the subsequent discovery of a second narrow particle, $D_{sJ}(2458)^+ \to D_s^*(2112)^+\pi^0$ [2,3,4] has raised considerable interest in the spectroscopy of heavy mesons. These discoveries have been a surprise because they contradict the expectations of a well established theory (Heavy Quark Effective Theory (HQET)).

A meson system made from one heavy and one light quark can be understood in a way analogous to the hydrogen atom [5]. This approach has been very successful in describing the spectroscopy of D, D_s, B and B_s mesons [6,7,8]. In this approach, the spin of the light quark couples with the orbital angular momentum L to make a conserved quantity $j = L \pm 1/2$. This in turn combines with the spin of the heavy quark to give total spin $J = j \pm 1/2$. The expected spectrum for $L = 1$ states is sketched in fig. 1. In this scheme both $j = 1/2$ and $j = 3/2$ contribute to $J = 1$.

A comparison between HQET calculations and experiment for D_s mesons is also shown in fig. 1. The two states with $j = 3/2$ are expected to be narrow and are most likely identified as the $J^P = 1^+$ $D_s(2536)$ and the $J^P = 2^+$ $D_{sJ}(2573)$ seen in D^*K and DK decays, respectively. Before the observations reported here became available, the two $j = 1/2$ states were predicted to have masses above the DK and D^*K threshods respectively, and with rather large widths. This would therefore

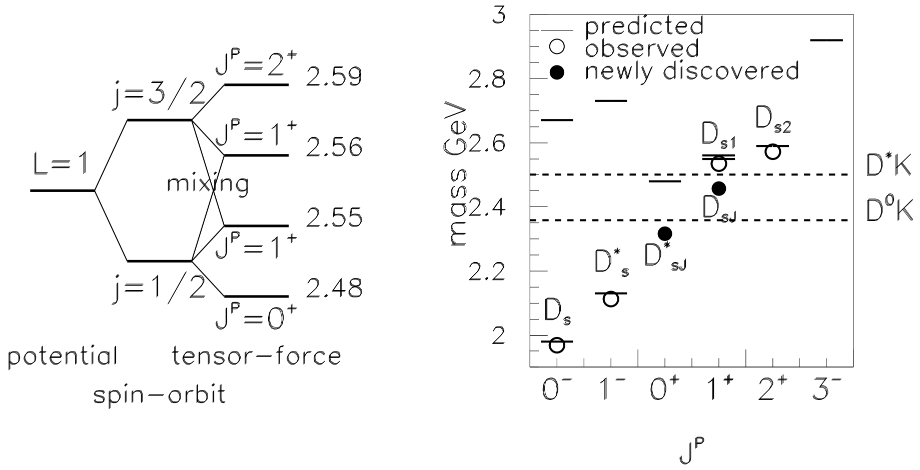

Fig. 1. P-wave states in the $c\bar{s}$ mesons multiplet according to the HQET scheme (left). Expectations on the masses of the $c\bar{s}$ mesons according to HQET calculations compared with experimental results (right).

make the missing states hard to detect.

It can be seen that the newly discovered states do not fit in this model. Their mass is consistently lower with respect to expectations and are below their relative thresholds, therefore extremely narrow (consistent with zero). Two possibilities then arise: the calculations are flawed, or these states have a quark composition other than $\bar{q}q$.

Experimentally, *BABAR* first discovered the $D^*_{sJ}(2317)^+$ particle, reporting also the presence of further structure in $D_{sJ}(2458)^+ \to D^*_s(2112)^+\pi^0$. This latter structure was, however, located on top of a set complex kinematic reflections which required a detailed study. In the mean time CLEO and Belle experiments confirmed the existence of both $D^*_{sJ}(2317)^+$ and $D_{sJ}(2458)^+$ particles in continuum and B decays.

This paper will mostly deal with experimental data from *BABAR* experiment.

2. The *BABAR* Experiment.

The *BABAR* detector (at the PEP-II asymmetric-energy e^+e^- storage ring with center-of-mass energy near 10.6 GeV) is a general purpose, solenoidal, magnetic spectrometer and is described in detail elsewhere [9]. The data sample used in this analysis corresponds to an integrated luminosity of 91 fb^{-1} collected between 1999 and 2002.

3. $D_s^+\pi^0$ events selection.

The objective of this analysis was to investigate the inclusively-produced $D_s^+\pi^0$ mass spectrum from continuum e^+e^- interactions.

For this purpose two identified charged kaons with opposite charge were combined with a charged pion requiring a common vertex from the decay $D_s^+ \to K^+K^-\pi^+$ [a]. π^0 candidates were reconstructed from a pair of photons and performing a one-constraint fit to the π^0 mass. A given event may yield several acceptable π^0 candidates; only those candidates for which neither photon belongs to another acceptable π^0 candidate were retained. To reduce combinatorial background from the continuum and eliminate background from B-meson decay, each $K^+K^-\pi^+\pi^0$ candidate was required to have a center-of-mass momentum p^* greater than 2.5 GeV/c.

The $K^+K^-\pi^+$ mass distribution for all candidates is shown in Fig. 2a) where clear peaks corresponding to D^+, D_s^+ and $D^{*+} \to \pi^+D^0(\to K^+K^-)$ mesons can be seen. Background from $D^0 \to K^+K^-$, which is evident from the corresponding K^+K^- mass distribution, was removed by requiring that the K^+K^- mass be less than 1.84 GeV/c^2.

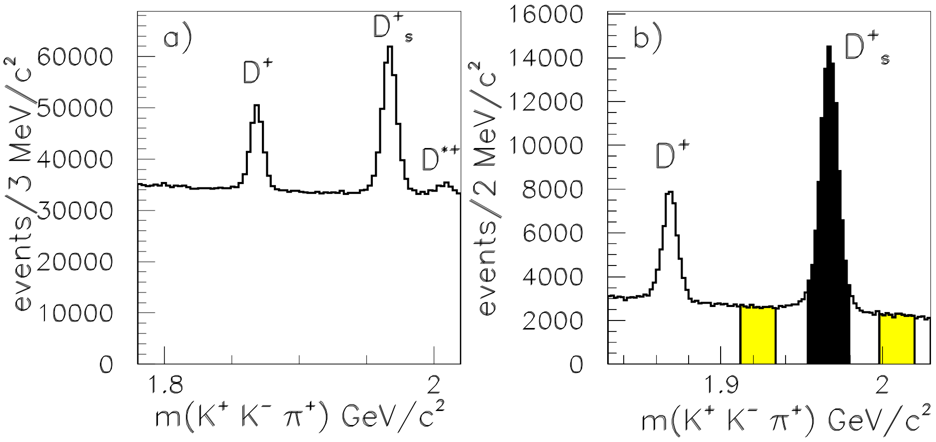

Fig. 2. a) The distribution of $K^+K^-\pi^+$ mass for all candidate events. b) $K^+K^-\pi^+$ mass distribution after having required the presence of ϕ and K^* resonances with further cuts on the angular distributions. The D_s^+ signal region is shown in black while sideband regions are shown shaded.

To reduce the background further, only those candidates with K^+K^- mass within 10 MeV/c^2 of the $\phi(1020)$ mass or with $K^-\pi^+$ mass within 50 MeV/c^2 of the

[a] The inclusion of charge-conjugate configurations is implied throughout this paper.

$\bar{K}^*(892)$ mass were retained. The decay products of the vector particles $\phi(1020)$ and $\bar{K}^*(892)$ exhibit the expected $\cos^2\theta_h$ behavior required by conservation of angular momentum, where θ_h is the helicity angle. The signal-to-background ratio is further improved by requiring $|\cos\theta_h| > 0.5$.

The resulting $K^+K^-\pi^+$ mass distribution is shown in Fig. 2b). The D_s^+ signal region is shown in black while sideband regions are shown shaded. The D_s^+ signal peak consists of approximately 80,000 events and is centered at a mass of (1967.20 ± 0.03) MeV/c^2.

Candidates in the D_s^+ signal region of Fig. 2b) are combined with the mass-constrained π^0 candidates to yield the mass distribution of Fig. 3. A clear, narrow signal of ≈ 2200 events at a mass near 2.32 GeV/c^2 is seen. The shaded histogram represents the events in the $D_s^+ \to K^+K^-\pi^+$ mass sidebands combined with the π^0 candidates where no signal is observed. This indicate that the new signal is associated to D_s^+.

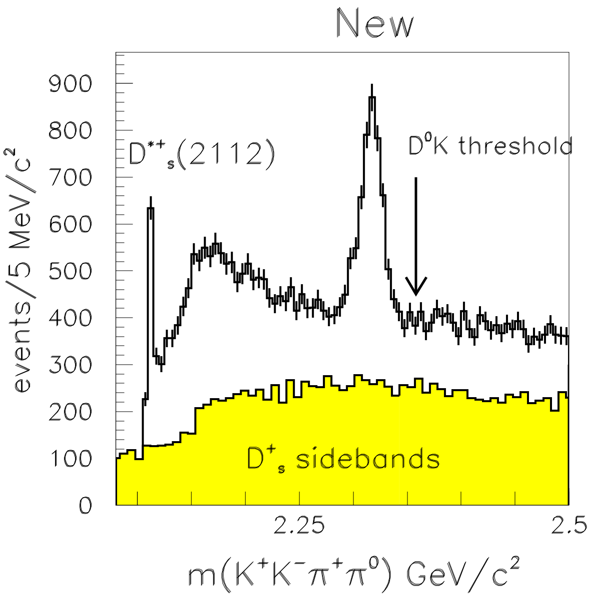

Fig. 3. The $D_s^+\pi^0$ mass distribution for candidates in the D_s^+ signal and $K^+K^-\pi^+$ sideband regions.

Figure 4 shows the mass distribution for all two-photon combinations associated with the selected events. The π^0 signal region is shown in black while sideband regions are shaded.

In Fig. 4b) the mass distributions result from the combination of the D_s^+ candidates with the photon pairs from the π^0 signal and sideband regions (the sideband distribution is again shaded). In Fig. 4b) the 2.32 GeV/c^2signal is absent from the

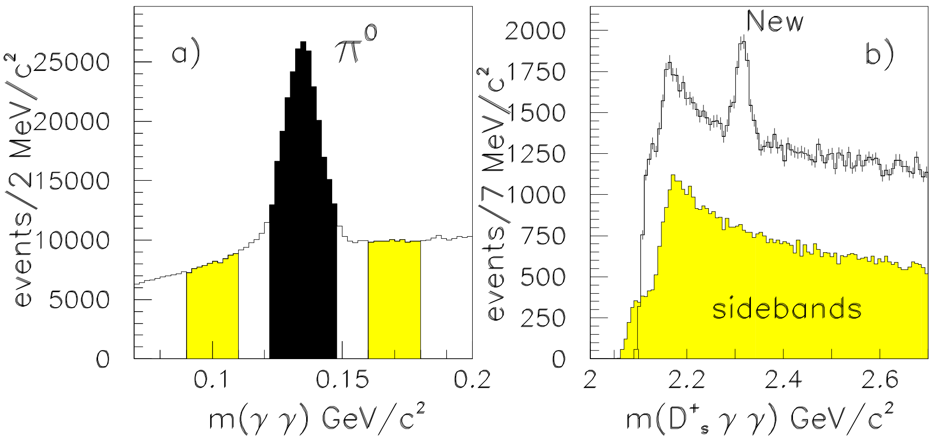

Fig. 4. a) Two-photon mass distribution from $D_s^+\pi^0$ candidate events. The π^0 signal and sideband regions are shaded. b) $D_s^+\gamma\gamma$ mass distribution for signal D_s^+ candidates and a photon pair from the π^0 signal region and the sideband regions.

sideband distributions indicating quite clearly that the peak is associated with the $D_s^+\pi^0$ system. In order to improve mass resolution, the nominal D_s^+ mass [10] was used to calculate the D_s^+ energy. It is also required that γ's from the π^0 are not shared with any other π^0 in the event ("π^0 veto").

The signal, labelled as $D^*_{sJ}(2317)^+$, is observed with similar strenghts in both the $\phi\pi^+$ and $\bar{K}^{*0}K^+$ decay modes of the D_s^+.

In order to inprove the signal to background ratio, the p^* cut was increased to 3.5 GeV/c yielding the mass spectrum shown in Fig. 5.

A first fit to this spectrum was performed using a Gaussian function describing the 2.32 GeV/c^2 signal and a polynomial background. The fit yields 1267 ± 53 candidates in the signal Gaussian with mass (2316.8 ± 0.4) MeV/c^2 and standard deviation (8.6 ± 0.4) MeV/c^2.

For reasons which will become clear later, the $D_s^+\pi^0$ mass spectrum was fitted a second time to incorporate the observation of $D_{sJ}(2458)^+$. Those results will be discussed later.

4. The $D^*_{sJ}(2317)^+$ from $D_s^+ \to K^+K^-\pi^+\pi^0$

As a cross check, *BABAR* selected a sample of $D_s^+ \to K^+K^-\pi^+\pi^0$ by adding π^0 candidates to each $K^+K^-\pi^+$ candidate. Fig. 6a) shows a clear D_s^+ signal on top of a large combinatorial background. Each resulting D_s^+ candidate was combined with a second π^0 candidate with lab momentum greater than 300 MeV/c. The "π^0 veto" request was also been applied. The center of mass momentum of the $K^+K^-\pi^+\pi^0\pi^0$ system was required to be greater that 3.5 GeV/c.

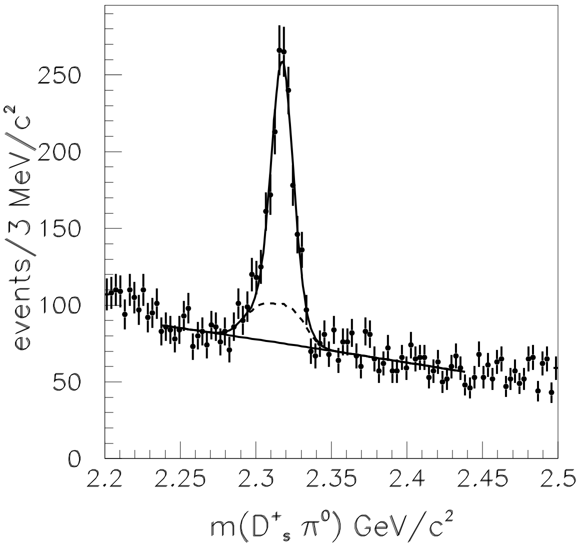

Fig. 5. a) $D_s^+\pi^0$ mass spectrum for $p^* > 3.5 GeV/c$ with superimposed the fit described in the text. The dashed line represents the estimated feedthrough from $D_{sJ}(2458)^+$.

The $D_s^+\pi^0$ mass distributions in the signal and sidebands region are shown in fig. 6b).

A clear $D^*_{sJ}(2317)^+$ signal was observed only in the signal region but not D_s^+ sidebands. A Gaussian fit yields 273 ± 33 events with a mean of (2317.6 ± 1.3) MeV/c^2 and width (8.8 ± 1.1) MeV/c^2. The mean and width are consistent with the values obtained for the $D_s^+ \to K^+K^-\pi^+$ decay mode indicating therefore that the observed structure was real. The mass distribution of the $D_s^+ \to K^+K^-\pi^+\pi^0$ sample peaks at (1967.4 ± 0.2) MeV/c^2.

Monte Carlo simulations were used to investigate the possibility that the $D^*_{sJ}(2317)^+$ signal could be due to reflection from other charmed states. This simulation included $e^+e^- \to c\bar{c}$ events and all known charm states and decays. The generated events were processed by a detailed detector simulation and subjected to the same reconstruction and event-selection procedure as that used for the data. No peak was found in the 2.32 GeV/c^2 $D_s^+\pi^0$ signal region.

Mass resolution estimates for the $K^+K^-\pi^+\pi^0$ system were obtained directly from the data using a fit to the mass distribution $D_s^+ \to K^+K^-\pi^+\pi^0$. The measured width from this mode is consistent with that of the $D^*_{sJ}(2317)^+$ signal. It can be concluded that the intrinsic width of the $D^*_{sJ}(2317)^+$ is small ($\Gamma \lesssim 10$ MeV).

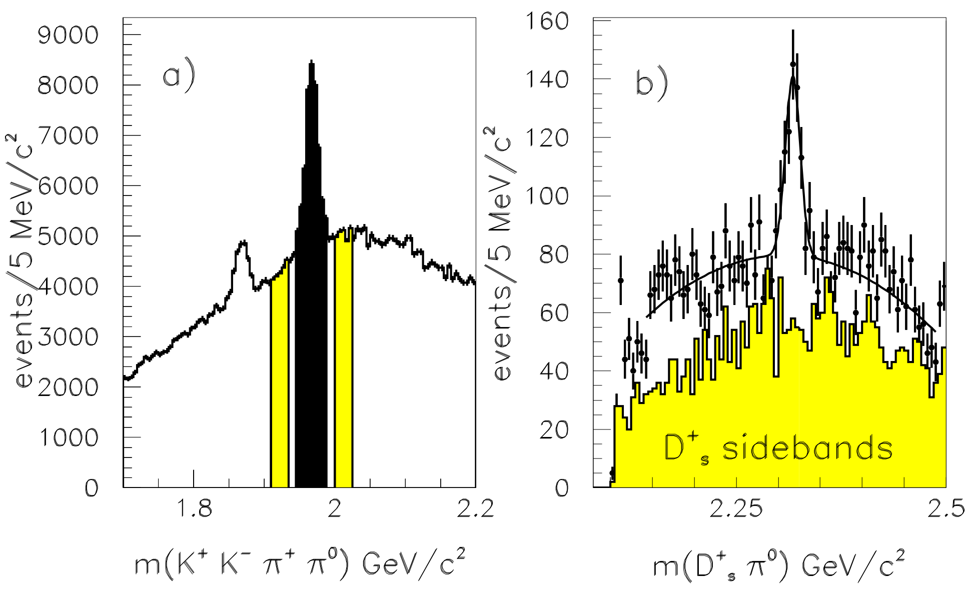

Fig. 6. a) $K^+K^-\pi^+\pi^0$ mass distribution. The signal region is shown in black while sideband regions are shown shaded; b) $D_s^+\pi^0$ mass distribution from the the decay $D_s^+ \to K^+K^-\pi^+\pi^0$. The shaded region is from D_s^+ sidebands.

5. Search for other $D_{sJ}^*(2317)^+$ decay modes.

A search was also performed for the decays $D_{sJ}^*(2317)^+ \to D_s^+\gamma$, $D_{sJ}^*(2317)^+ \to D_s^+\gamma\gamma$ and $D_{sJ}^*(2317)^+ \to D_s^*(2112)^+\gamma$.

Shown in Fig. 7a) is the $D_s^+\gamma$ mass distribution obtained by combining a D_s^+ candidate in the signal region of Fig. 2b) with a photon with an energy of at least 150 MeV that does not belong to a $\gamma\gamma$ combination in the signal region of Fig. 4a). The requirement that the p^* of the $D_s^+\gamma$ system be greater than 3.5 GeV/c was also imposed.

There is a clear $D_s^*(2112)^+$ signal, but no indication of $D_{sJ}^*(2317)^+$ production.

The $D_s^+\gamma\gamma$ mass distribution for $p^*(D_s^+\gamma\gamma) > 3.5$ GeV/c, excluding any photon that belongs to the π^0 signal region is shown as the upper histogram of Fig. 7b). No signal is observed near 2.32 GeV/c^2. The shaded histogram corresponds to the subset of combinations for which either $D_s^+\gamma$ combination lies in the $D_s^*(2112)^+$ region, defined as $2.096 < m(D_s^+\gamma) < 2.128$ GeV/c^2. Again, no $D_{sJ}^*(2317)^+$ signal is evident, thus demonstrating the absence of a $D_s^*(2112)^+\gamma$ decay mode at the present level of statistics.

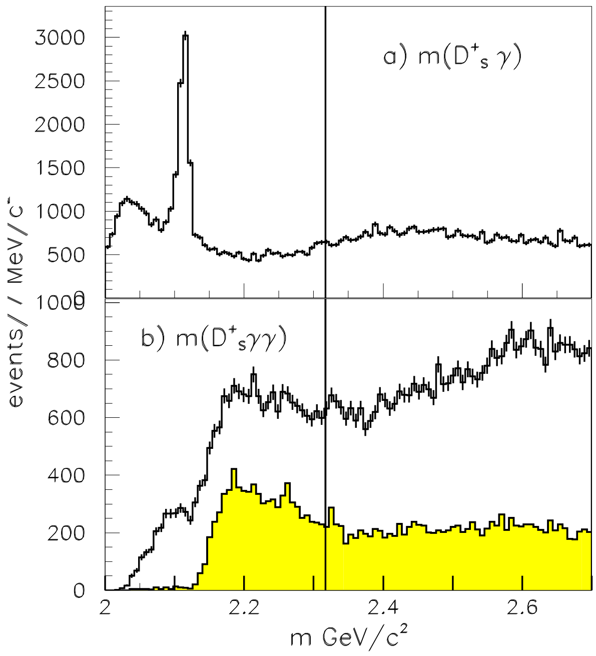

Fig. 7. The mass distribution for a) $D_s^+\gamma$ and b) $D_s^+\gamma\gamma$ after excluding photons from π^0's. The shaded histogram includes the request that either $D_s^+\gamma$ lies in the $D_s^*(2112)^+$ region.

6. Study of the $D_s^+\pi^0\gamma$ system and the observation of $D_{sJ}(2458)^+$.

In order to study the $D_s^+\pi^0\gamma$ system, each D_s^+ candidate was combined with all combinations of accompanying π^0 candidates with momentum greater than 300 MeV/c and photon candidates of energy greater than 100 MeV/c^2. To suppress background the "π^0 veto" was applied and the combined momentum p^* in the e^+e^- center-of-mass mass frame of each $D_s^+\pi^0\gamma$ combination was required to be greater than 3.5 GeV/c. The $D_s^+\pi^0\gamma$ mass spectrum resulting from this selection is shown in fig. 8a) where a narrow signal in the region of 2.46 GeV/c^2 on top of a large background. No structure was observed in the D_s^+ sideband region. No evidence was found for a $D_{sJ}^*(2317)^+$ decay to $D_s^+\pi^0\gamma$.

The background underneath this peak is from several sources, which can be described in terms of mass differences defined as:

$$\Delta m(D_s^+\gamma) \equiv m(K^-K^+\pi^+\gamma) - m(K^-K^+\pi^+) \tag{1}$$

$$\Delta m(D_s^{*+}\pi^0) \equiv m(K^-K^+\pi^+\pi^0\gamma) - m(K^-K^+\pi^+\gamma)\ . \tag{2}$$

A scatter plot of these quantities is plotted in Fig. 8b). Two signals are clearly visible: $D_s^*(2112)^+ \to D_s^+\gamma$ decay combined with unassociated π^0 candidates, which appears as a horizontal band, and $D_{sJ}^*(2317)^+ \to D_s^+\pi^0$ decay combined with unas-

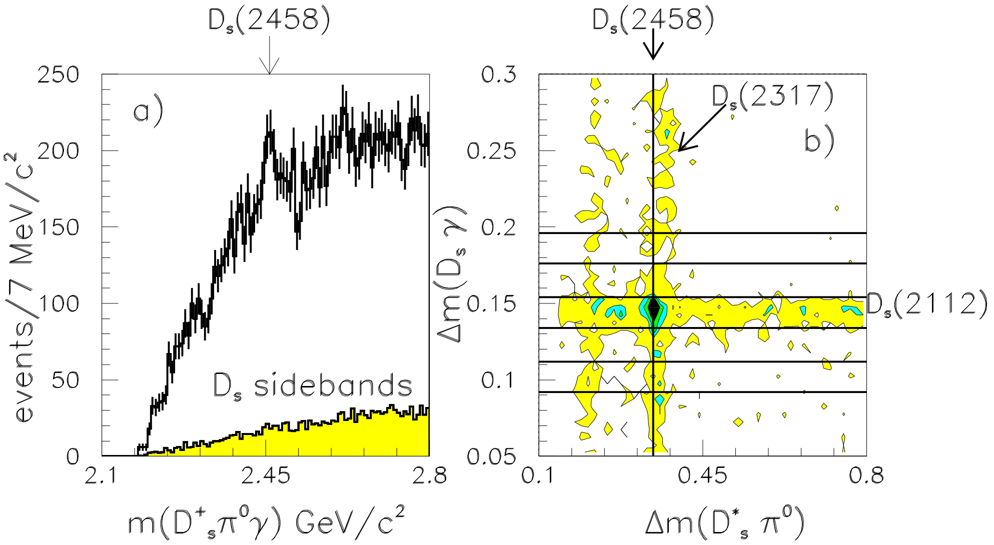

Fig. 8. a) $D_s^+\pi^0\gamma$ mass distribution.The shaded histogram is from D_s^+ sidebands. b) The value of $\Delta m(D_s^+\gamma)$ versus $\Delta m(D_s^{*+}\pi^0)$ for all combinations. The horizontal lines delineate three ranges in $\Delta m(D_s^+\gamma)$.

sociated γ candidates, which appears as a band that is almost vertical.

An enhancement associated with the $D_{sJ}(2458)^+$ is evident in the vicinity of the overlap of these two bands with a $D_s^+\pi^0\gamma$ mass near 2.46 GeV/c^2. The histogram of Fig. 9a) shows events in the $D_s^*(2112)^+$ signal region, and the shaded histogram shows those in the two $D_s^*(2112)^+$ sidebands. One can conclude that a state with decay to $D_s^+\pi^0\gamma$ is seen to exist over a background from $D_{sJ}^*(2317)^+$ combined with a γ. This background is peaked at a mass slightly higher than the signal (≈ 5 MeV/c). In Fig. 9b) the subtracted plot shows the narrow signal fitted to a Gaussian shape on a second order polynomial background at $\Delta m(D_s^+\gamma) = 346.2\pm0.9\,\mathrm{MeV}/c^2$. Fig. 9c) shows the effect of removing the π^0 veto: the contribution to the $D_{sJ}(2458)^+$ signal from $D_{sJ}^*(2317)^+$ is clearly larger.

To obtain the final state $D_s^+\pi^0\gamma$, the $D_{sJ}(2458)^+$ may decay through two intermediate resonant states, $D_s^*(2112)^+\pi^0$ or $D_{sJ}^*(2317)^+\gamma$. To disentangle these modes and reliably extract the parameters of the signal, *BABAR* applied an unbinned maximum likelihood fit simultaneously to the $D_s^+\pi^0\gamma$, $D_s^+\pi^0$, and $D_s^+\gamma$ invariant masses of all $D_s^+\pi^0\gamma$ combinations using the channel likelihood method [11]. This fit described the probability density function of the two $D_{sJ}(2458)^+$ decay channels as the product of a Gaussian shape in the $D_s^+\pi^0\gamma$ mass distribution and a Gaussian shape projected into the $D_s^+\pi^0$ or $D_s^+\gamma$ mass axes, as appropriate. Because the daughter resonances are narrow, interference between the two $D_{sJ}(2458)^+$ decay modes cannot be resolved, and so it was ignored.

Sources of background in the $D_s^+\pi^0\gamma$ spectrum included in the fit were purely

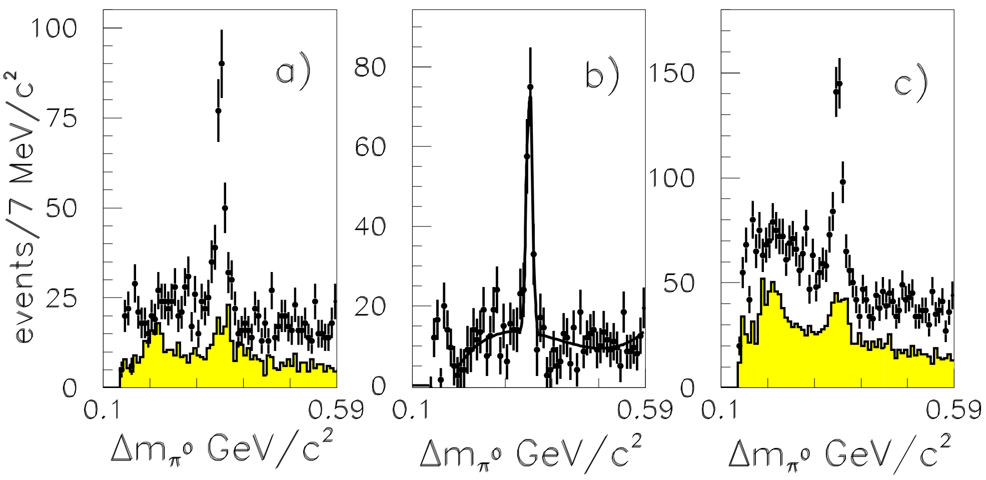

Fig. 9. a) The $\Delta m(D_s^{*+}\pi^0)$ mass distribution for the middle range of $\Delta m(D_s^+\gamma)$ (white) and for the upper and lower ranges (shaded). b) The difference of the two histograms shown in a). The curve is the fit described in the text. c) Same as a) but relaxing the condition of the "π^0 veto".

combinatorial background (D_s^+ meson combined with an unassociated π^0 and γ), $D_s^*(2112)^+ \to D_s^+\gamma$ decay combined with an unassociated π^0, and $D_{sJ}^*(2317)^+ \to D_s^+\pi^0$ decay combined with an unassociated γ. The fit also included a contribution from $D_{sJ}(2458)^+ \to D_s^*(2112)^+\pi^0$ decay but with an unassociated γ replacing the γ from $D_s^*(2112)^+$ decay. The fit determined the relative size of the background and signal contributions, the mass and width of the $D_{sJ}(2458)^+$, and the $D_{sJ}^*(2317)^+$ mass.

As shown in Fig. 10a, the fit provides a good description of the $D_s^+\pi^0\gamma$ mass distribution. The $D_{sJ}(2458)^+$ signal, for a particular decay mode can be isolated by calculating a weight for each $D_s^+\pi^0\gamma$ combination proportional to the relative likelihood contributed by the decay mode of interest. Distributions of events so weighted can be compared to the likelihood function to validate the fit. This is shown in Figs. 10b) and 10c).

The resulting yield of correctly reconstructed $D_{sJ}(2458)^+ \to D_s^*(2112)^+\pi^0$ ($D_{sJ}(2458)^+ \to D_{sJ}^*(2317)^+\gamma$) decays was 195 ± 26 (0 ± 23), consistent with the fit shown in Fig. 9b). Excluding the $D_{sJ}(2458)^+$ from the likelihood fit decreased the log likelihood by approximately 57, corresponding to a significance of more than 10 standard deviations.

The fit yielded a $D_{sJ}(2458)^+$ mass of 2458.0 ± 1.0 MeV/c^2 with an rms width of 8.5 ± 1.0 MeV/c^2.

Monte Carlo simulations have been used to estimate the detector resolution,

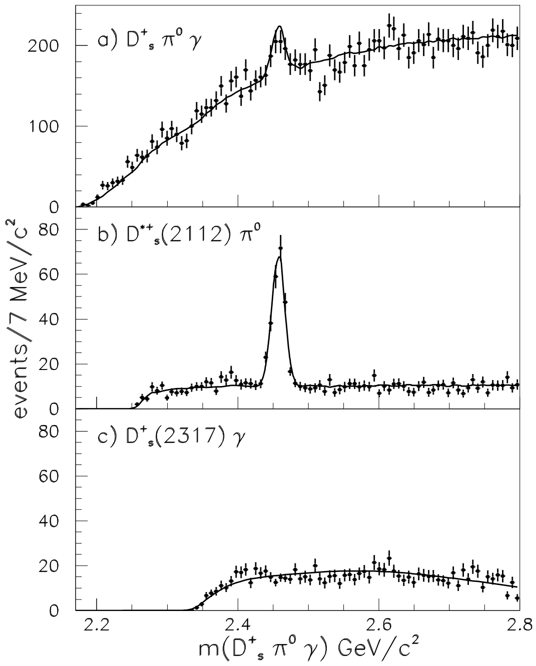

Fig. 10. Maximum likelihood fit results overlaid on the $D_s^+\pi^0\gamma$ mass distribution with a) no weights and after applying weights corresponding to b) the decay $D_s^*(2112)^+\pi^0$ and c) the decay $D_{sJ}^*(2317)^+\gamma$.

leading to the conclusion that the intrinsic width of the $D_{sJ}(2458)^+$ is small ($\Gamma \lesssim 10$ MeV/c^2).

The previous determination of the $D_{sJ}^*(2317)^+$ mass using the decay $D_{sJ}^*(2317)^+ \to D_s^+\pi^0$ did not explicitly consider background from $D_{sJ}(2458)^+ \to D_s^*(2112)^+\pi^0$ decay. This background peaks in the $D_s^+\pi^0$ mass spectrum just below the $D_{sJ}^*(2317)^+$ mass. Refitting the mass spectrum shown in fig. 5 including the contribution from the $D_{sJ}(2458)^+$ as estimated from MC simulation results in a $D_{sJ}^*(2317)^+$ yield of 1022 ± 50 events, a mass of 2317.3 ± 0.4 MeV/c^2, and measured rms width 7.3 ± 0.2 MeV/c^2.

The resulting total systematic uncertainty in the $D_{sJ}(2458)^+$ [$D_{sJ}^*(2317)^+$] mass is ±1.0 [±0.8] MeV/c^2.

Using the yields from the fit and correcting for efficiency, *BABAR* estimated the relative production rate

$$R = \frac{\sigma(D_{sJ}(2458)^+)\mathcal{B}(D_{sJ}(2458)^+ \to D_s^*(2112)^+\pi^0)}{\sigma(D_{sJ}^*(2317)^+)\mathcal{B}(D_{sJ}^*(2317)^+ \to D_s^+\pi^0)} \tag{3}$$

to be $0.25 \pm 0.03(stat.) \pm 0.03(syst)$, requiring $p^* > 3.5$ GeV/c for both states.

They also estimated, at 95% C.L.,

$$\frac{\mathcal{B}(D_{sJ}(2458)^+ \to D_{sJ}^*(2317)^+\gamma)}{\mathcal{B}(D_{sJ}(2458)^+ \to D_s^*(2112)^+\pi^0)} < 0.22\ . \tag{4}$$

7. Results from CLEO and Belle.

Using 13.5 and 86.9 fb^{-1} integrated luminosity, the CLEO [2] and Belle [3] experiments confirmed the existence of $D_{sJ}^*(2317)^+$. In terms of Δm, CLEO reported a value of $\Delta m = 350.3 \pm 1.2$ MeV/c^2 with 155 ± 23 events. Belle reported $\Delta m = 348.7 \pm 0.5$ MeV/c^2 with 761 ± 44 events. These values are in good agreement with the *BABAR* measurement of $\Delta m = 348.4 \pm 0.4$ MeV/c^2. Both experiments made use, in their analysis, only of the $D_s^+ \to \phi\pi^+$ decay mode.

In addition, both the CLEO and Belle Collaborations have analyzed the $D_s^*(2112)^+\pi^0$ mass distribution finding evidence for structure in the 2.46 GeV region. They reported the following parameters for this state: Δm=351.2 $\pm$ 1.7 MeV/c^2 with 41 ± 12 events (CLEO) and Δm=344.1 $\pm$ 1.3 MeV/c^2 with 79 ± 18 events (Belle).

The result from CLEO gives a somewhat larger value for the mass of $D_{sJ}^*(2317)^+$. A possible explanation is that their analysis did not make use of a "π^0 veto". This increases the contamination in the $D_{sJ}(2458)^+$ signal from $D_s^*(2112)^+\pi^0$ background which peaks approximately 5 MeV/c^2 higher.

Belle analysis, on the other hand, did not consider explicitely the possibility of a $D_{sJ}(2458)^+$ decay to $D_{sJ}(2458)^+ \to D_{sJ}^*(2317)^+\gamma$.

The measured production rate from the two experiments is $R = 0.44 \pm 0.13$ (CLEO) and $R = 0.26 \pm 0.05$ (Belle) respectively. The *BABAR* result is in agreement with that from Belle but somewhat smaller with respect to CLEO measurement.

Belle also reported observation of both states [12] in the B decays to $B \to DD_{sJ}^*(2317)^+$ and $B \to DD_{sJ}(2458)^+$. In addition, they reported the observation of $D_{sJ}(2458)^+ \to D_s^+\gamma$ in both B decays and continuum e^+e^- annihilations (see fig. 11). The angular analysis showed the expected behaviour for a $J^P = 1^+$ state. Belle has also reported on the observation of the decay $D_{sJ}(2458)^+ \to D_s^+\pi^+\pi^-$.

No evidence has been reported up to now for narrow structures in $D_s^+\pi^\pm$ final states.

8. Discussion and conclusions

The two new states do not follow the pattern expected from HQET calculations. The mass of $D_{sJ}^*(2317)^+$ is 40.8 MeV below the D^0K threshold. The low mass and the absence of a $D_{sJ}^*(2317)^+ \to D_s^+\gamma$ favors $J^P = 0^+$ for $D_{sJ}^*(2317)^+$. The mass of $D_{sJ}(2458)^+$ lies above the DK threshold and 41.5 MeV below D^*K threshold.

The decay of any $c\bar{s}$ state to $D_s^+\pi^0$ or $D_s^*(2112)^+\pi^0$ violates isospin conservation, thus guaranteeing a small width for these states. It is possible that the decays proceeds via $\eta - \pi^0$ mixing, as discussed by Cho and Wise [13].

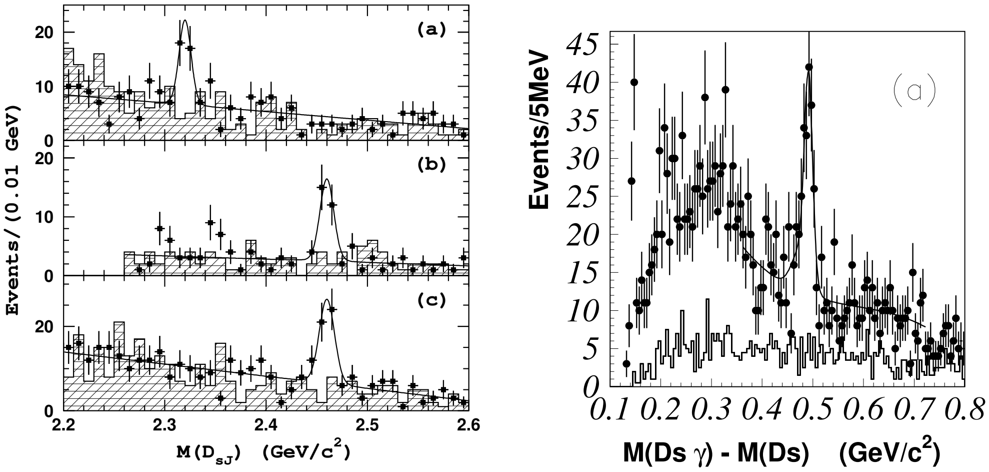

Fig. 11. Left: observation of $D^*_{sJ}(2317)^+ \rightarrow D_s^+\pi^0$, $D_{sJ}(2458)^+ \rightarrow D_s^*(2112)^+\pi^0$ and $D_{sJ}(2458)^+ \rightarrow D_s^+\gamma$ in B decays from Belle. Right: observation of $D_{sJ}(2458)^+ \rightarrow D_s^+\gamma$ in continuum e^+e^- annihilations from Belle.

The failure of quark potential models to explain such low masses for these new particles has triggered a large number of phenomenological papers [14]. A few of these papers are discussed below.

Cahn and Jackson [15] interpret the new states in terms of relativistic vector and scalar exchange forces. Godfrey [16] and Colangelo and De Fazio [17] predict significant $D^*_{sJ}(2317)^+$ radiative decays under the hypothesis these states are $c\bar{s}$ mesons.

Van Beveren and Rupp [19] explain the $D^*_{sJ}(2317)^+$ as a quasi-bound scalar $c\bar{s}$ state in a unitarized meson model, similar to other light scalar mesons. Barnes, Close and Lipkin [18] propose DK molecular states, K. Terasaki [22] four-quark states, while Szczepaniak [21] suggests a $D\pi$ atom.

Bardeen, Eichten and Hill [20] uses HQET plus chiral symmetry to predict parity doubling, i.e. the expectation is that the mass splitting between the 1^+ and 1^- states should be the same as for the 0^+ and 0^- states.

Bali [23] reports lattice QCD calculations which produce masses for the 0^+ and 1^+ states higher than those experimentally measured.

In conclusion, the discovery of these new mesons with unexpected properties have opened a new window in spectroscopy and current models of charm meson spectroscopy most likely need modification.

Acknowledgments

I would like to thank the *BABAR* collaboration for the opportunity to partecipate to this fantastic scientific adventure. In particular I would like to thank the collaboration with D. Williams, W. Dunwoodie, B. Meadows, J. Bartelt, W. Lockman, R. Cahn and A. Snyder.

This work is supported by the University of Bari and the Istituto Nazionale di Fisica Nucleare (Italy),

References

1. B. Aubert *et al*, (BaBar Collaboration) Phys. Rev. Lett. **90**, 242001 (2003).
2. D. Besson *et al* (CLEO Collaboration), Phys. Rev. **D68**, 032002 (2003).
3. K. Abe *et al* (Belle Collaboration), Phys. Rev. Lett. **92**, 012002 (2004).
4. B. Aubert *et al*, (BaBar Collaboration) Phys. Rev. **D69**, 031101 (2004).
5. A. De Rujula, H. Georgi, and S.L. Glashow, Phys. Rev. Lett. **37**, 785 (1976).
6. S. Godfrey and N. Isgur, Phys. Rev. **D32**, 189 (1985).
7. S. Godfrey and R. Kokoski, Phys. Rev. **D43**, 1679 (1991).
8. M. Di Pierro and E. Eichten, Phy. Rev. **D64**, 114004 (200 1).
9. B. Aubert *et al*, Nucl. Instrum. Meth. **A479**, 1 (2002).
10. K. Hagiwara *et al*, (Particle Data Group) Phys. Rev. **D66**, 010001 (2001).
11. P. E. Condon and P. L. Cowell, Phy. Rev. **D9**, 2558 (1974).
12. K. Abe *et al* (Belle Collaboration), Phys. Rev. Lett. **91**, 262002 (2003).
13. P.L. Cho and M.B. Wise, Phys. Rev. **D49**, 6228 (1994).
14. W. Lucha and F.S. Schöberl, Modern Phys. Lett. A **18** 2837 (2003).
15. R.N. Cahn and J.D. Jackson, hep-ph/0305012.
16. S. Godfrey, hep-ph/0305122.
17. P. Colangelo and F. De Fazio, hep-ph/0305140.
18. T. Barnes, F.E. Close and H.J. Lipkin, hep-ph/0305025.
19. E. van Beveren and G. Rupp, hep-ph/0305035.
20. W.A. Bardeen, E.Eichten and C.T. Hill, hep-ph/0305049.
21. A.P. Szczepaniak, hep-ph/0305060.
22. K. terasaki, hep-ph/0305213.
23. Gunnar S. Bali, hep-ph/0305209.